Copper(II)-assisted self-assembly of bis-*N*,*O*-bidentate Schiff bases: new building blocks for a double-helical supramolecular motif

Noboru Yoshida,*[a] Hiroki Oshio[b] and Tasuku Ito[b]

[a] *Laboratory of Molecular Functional Chemistry, Division of Material Science, Graduate School of Environmental Earth Science, Hokkaido University, Sapporo 060, Japan*
[b] *Department of Chemistry, Graduate School of Science, Tohoku University, Sendai 980-77, Japan*

Received (in Cambridge) 15th December 1998, Accepted 22nd February 1999

Copper(II)-assisted self-assembly of a new bis-*N*,*O*-bidentate Schiff base ligand, bis(*N*-salicylidene-3,3′-diaminodiphenyl) sulfone (**L**[1]) with two chelating sites linked by a spacer group (-$C_6H_4SO_2C_6H_4$-), afforded in high yield the double-helical tetranuclear supramolecular complex with eight components. Single-crystal X-ray analyses demonstrated clearly that two Cu^{II} centers have a distorted tetrahedral (T_d) coordination sphere, whereas the other two remaining Cu^{II} have a square-planar coordination sphere. An analogous Schiff base, bis(*N*-salicylidene-4,4′-diaminodiphenyl) ether (**L**[6]) with a phenyl ether spacer (-$C_6H_4OC_6H_4$-) was also designed to self-assemble in the presence of metal ions, leading to a double-helical dinuclear supramolecular motif. Electrospray mass spectrometry proved a very useful characterizational tool to detect a variety of supramolecular species in solution. These unprecedented double-helical motifs in solid and solution seem to be induced by the geometrical preference for tetrahedral and/or square-planar coordination of copper(II) ion and the interligand aromatic interactions between the bridging groups of **L**[1] and **L**[6].

Introduction

Noncovalent interactions such as hydrophobic bonds, van der Waals forces, and hydrogen bonds play an important role in the formation of host–guest complexes[1] and supramolecular architectures[2] in solution.

A recent attractive application of aromatic π–π and CH · · · π interactions[2a,3] is a general synthetic method for the construction of many types of supramolecular motifs.[4,5] Some metal ions such as Cu^{I}[6] and Ag^{I} with a specific geometrical preference have often been used in order to assist the formation of organized structures by self-assembly of target ligands. Double-helical,[7] triple-helical,[8] toroidal,[9] cylindrical,[10] molecular-size boxed,[11] and circular[12] multinuclear structures have been generated by the complexation of rigid oligomultidentate ligands with two or more metal ions. However, the relationships between the effect of the noncovalent bond on the structure and the role of the metal ion in the self-assembly of ligands are not always clear.

Development of simple synthetic methods in the self-assembling process using commercially available starting materials is also important to extend the wide range of different supramolecular structures in solution.[4,5] From this synthetic strategy, we have focused on some semi-*N*,*O*-bidentate and bis-*N*,*O*-bidentate Schiff base ligands which can be electronically and configurationally controlled, leading to a systematic study of the self-assembly process in solution.[5,13]

Here, we report a novel and general strategy for the construction of copper(II)-assisted supramolecular architectures of bis-*N*,*O*-bidentate Schiff bases, **L**[1] and **L**[6] (Scheme 1). These Schiff base ligands contain two *N*,*O*-bidentate chelating sites separated by a flexible bridging group such as -$C_6H_4SO_2C_6H_4$- or -$C_6H_4OC_6H_4$-. These ligands are designed to bind two separated metal ions by two sites because the bridging group does not allow one metal center to be ligated in a tetradentate fashion. The double-helical multinuclear structures which were confirmed by X-ray crystallography appear to be formed mainly due to two factors: the unique coordination geometry of

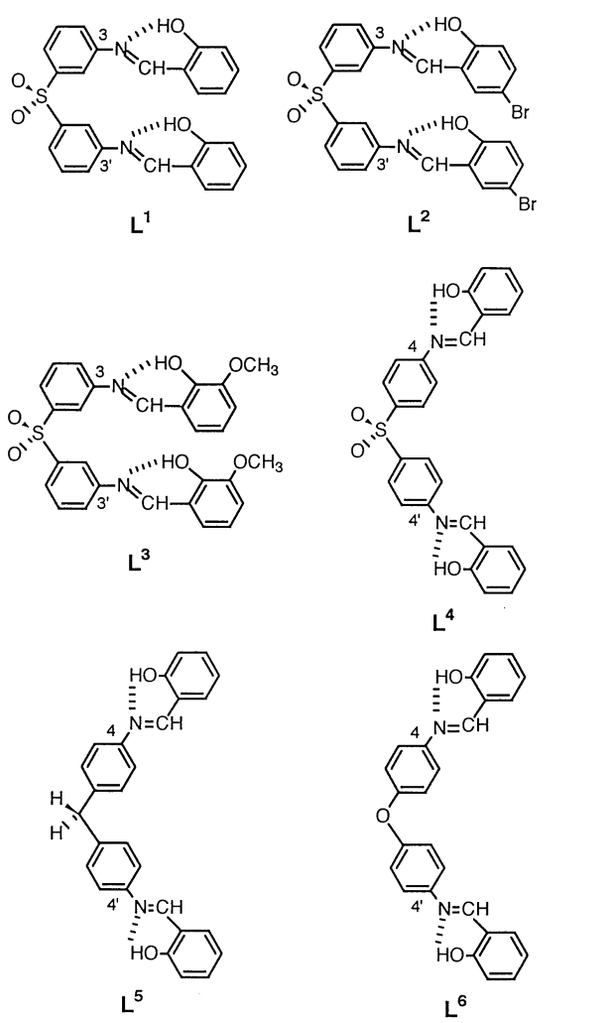

Scheme 1

Cu^{II} ion and the weak aromatic $\pi\cdots\pi$ and $CH\cdots\pi$ interactions between the spacer groups in $\mathbf{L^1}$ and $\mathbf{L^6}$.

Experimental

Preparations of ligands and Cu^{II} complexes

The Schiff base $\mathbf{L^1}$ was synthesized using the usual condensation [14] in ethanol of bis(3-aminophenyl) sulfone (0.5 mol) with salicylaldehyde (1 mol). The solution was stirred for 30 min at 60 °C. An orange colored solid precipitate was collected by filtration.

Data for the bis-bidentate Schiff base $\mathbf{L^1}$: Pale orange crystalline powder, 85% yield (Found: C, 67.75; H, 4.42; N, 6.14; S, 7.02%. $C_{26}H_{20}N_2O_4S$ requires C, 68.40; H, 4.41; N, 6.13; S, 7.02%), ^{1}H NMR (400 MHz, $CDCl_3$ in a small amount of NEt_3, internal reference TMS): δ 12.66 (2H, s, OH$\cdots$N), 8.65 (2H, s, CH=N), 7.90–7.84 (4H, m, aminophenyl H^2 and H^6), 7.59 (2H, td, J = 7.8, 0.9, aminophenyl H^5), 7.48 (2H, ddd, J = 7.8, 1.8, 0.9, aminophenyl H^4), 7.43 (2H, d, J = 7.3, salicylaldehyde (sal-ald) H^6), 7.42 (2H, td, J = 7.3, 1.5, sal-ald H^4), 7.03 (2H, d, J = 7.8, sal-ald H^3), and 6.97 (2H, td, J = 7.3, 1.0, sal-ald H^5). The ligand $\mathbf{L^6}$ is also prepared by the same synthetic method (pale yellow crystalline powder, 80% yield, Found: C, 76.39; H, 5.05; N, 6.89%. $C_{26}H_{20}N_2O_3$ requires C, 76.45; H, 4.93; N, 6.85%), ^{1}H NMR (400 MHz, $CDCl_3$ in a small amount of NEt_3, internal reference TMS): δ 13.23 (2H, s, OH$\cdots$N), 8.64 (2H, s, CH=N), 7.42–7.36 (4H, m, sal-ald H^4 and H^6), 7.31 (4H, ddd, J = 8.8, 3.4, 2.0, aminophenyl H^2 or H^3), 7.09 (4H, ddd, J = 8.8, 3.4, 2.0, aminophenyl H^2 or H^3), 7.03 (2H, d, J = 8.3, sal-ald H^3), 6.95 (2H, td, J = 7.6, 1.0, sal-ald H5). Other ligands, $\mathbf{L^2}$–$\mathbf{L^5}$, were also prepared by the same synthetic method.

Reaction of $\mathbf{L^1}$ with Cu(II) acetate hydrate in a 1:1 molar ratio in hot EtOH gave a light green solid. An equimolar mixture of $\mathbf{L^1}$ (0.78 g, 1.72 mmol) and $Cu(CH_3COO)_2\cdot H_2O$ (0.34 g, 1.7 mmol) in EtOH (100 ml) was heated at *ca.* 50 °C for 2 h. After cooling, a green powder was formed and collected by filtration (yield *ca.* 70–80%, Found: C, 60.66; H, 3.64; N, 5.46; S, 6.11%. $C_{52}H_{36}N_4O_8S_2Cu_2$ requires C, 60.28; H, 3.50; N, 5.40; S, 6.18%). This powder can be easily dissolved in DMF and chloroform. X-Ray quality crystals (dark brown) of **1** were obtained by the diffusion of ether into the chloroform solution of the complex. Elementary analysis suggests a 1:1 (metal:ligand) ratio and field desorption (FD) mass spectroscopy (FD-MS) implies the formation of a Cu^{II}:$\mathbf{L^1}$ = 2:2 complex. However, electrospray ionization mass spectrometry (ESI-MS) suggests strongly the existence of 3:3 and 4:4 complexes in addition to the 2:2 complex. Its electronic absorption spectrum shows a π–π* band at 400 nm in the visible region which shows the deprotonation of the OH group [14] and the *N*,*O*-coordination to Cu^{II}. Other metal complexes with Zn^{II}, Ni^{II} and Co^{II} prepared in the same synthetic conditions are insoluble in most common organic solvents, which suggests the formation of $(1:1)_\infty$ polymeric structures. A dark brown solid (50% yield, Found: C, 65.37; H, 3.57; N, 5.92%. $C_{52}H_{36}N_4O_6Cu_2$ requires C, 66.44; H, 3.86; N, 5.96%) for the Cu^{II} complex of $\mathbf{L^6}$ was obtained in the same conditions except for the solvent (DMF) and temperature (room temp.). Single crystals of complex **2** suitable for X-ray crystallography were obtained by slow evaporation of the $CHCl_3$ solution of Cu^{II}–$\mathbf{L^6}$.

Single crystal X-ray structure analysis

Precise data collection and crystal parameters for **1** are reported in Table 1. A single crystal of **1** was mounted on a glass fiber with epoxy resin. Diffraction data were collected at −100 °C on a Rigaku AFC 7S equipped with graphite monochromated Mo-Kα radiation (λ = 0.71073 Å). The structure was solved by direct methods with SHELX-86 (G. M. Sheldrick, University of Göttingen, 1986) and Fourier techniques, and refined by full-matrix least-squares on F^2 data using SHELXL-93 (G. M. Sheldrick, University of Göttingen, 1993), and converged at R_1 = 0.0667, wR_2 = 0.1652.† Crystal data for **2** are also shown in Table 1.

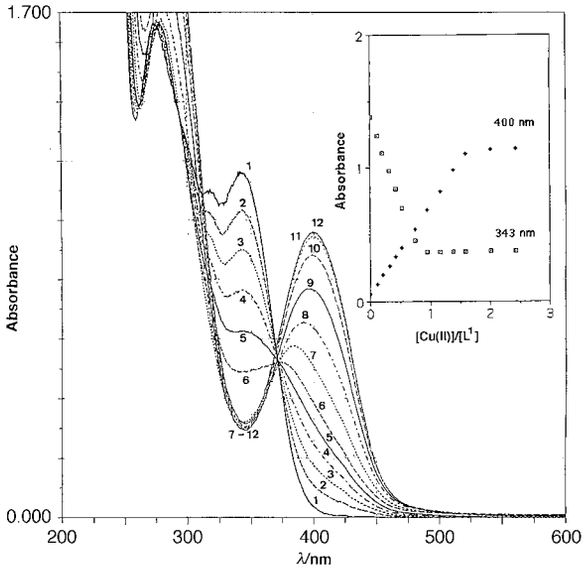

Fig. 1 Absorption spectral change of ligand $\mathbf{L^1}$ in ethanol upon addition of $Cu(CH_3COO)_2\cdot H_2O$. $[\mathbf{L^1}] = 6.48 \times 10^{-5}$ mol dm^{-3}. $[Cu^{II}] = 0$, 0.687, 1.37, 2.06, 2.747, 3.43, 4.80, 6.18, 7.55, 8.92, 10.3, 13, 15.8×10^{-5} mol dm^{-3}. The spectrum for **1** coincides with the spectrum at λ_{max} = 379.5 nm (the corresponding spectrum is No. 7 from the bottom at $[Cu^{II}]/[\mathbf{L^1}] = 1$).

Results and discussion

Electronic absorption spectra of the Cu^{II} and Zn^{II} complexes with $\mathbf{L^1}$

Fig. 1 shows the change in the uv–vis spectrum which occurs when $\mathbf{L^1}$ coordinates to Cu^{II} ion in EtOH. Upon addition of Cu^{II} ion to the ligand solution, the ligand π–π* band at 343 nm decreases, and a new band at 400 nm due to the deprotonation of the OH group [15] and the *N*,*O*-coordination to Cu^{II} ion emerges. A mole ratio plot using the change in absorbance at 343 nm clearly demonstrated the formation of the Cu^{II}:$\mathbf{L^1}$ = 1:1 molar ratio complex, as judged by observing the clear inflection point at $[Cu^{II}]/[\mathbf{L^1}] = 1$. However, further additions of Cu^{II} ion lead to an additional increase in the absorbance at 400 nm and a saturation at $[Cu^{II}]/[\mathbf{L^1}]$ = *ca.* 1.5 (the inset in Fig. 1). In addition, the isosbestic point at 375 nm shifts gradually to a shorter wavelength. The plateauing at two different $Cu^{II}/\mathbf{L^1}$ ratios suggests structure switching at the higher Cu^{II} concentration. The corresponding changes in the Zn^{II}–$\mathbf{L^1}$ system show several isosbestic points at 250, 323, 375 nm and their saturations take place at a ratio of exactly $[Zn^{II}]/[\mathbf{L^1}] = 2$.

It is noteworthy that strong fluorescence (*ca.* 140 times as compared with $\mathbf{L^1}$) is observed in the Zn(II) complex formation with $\mathbf{L^1}$.‡ Fluorescence intensity (λ_{ex} = 350 nm and λ_{em} = 500

† Full crystallographic details, excluding structure factor tables, have been deposited at the Cambridge Crystallographic Data Centre (CCDC). For details of the deposition scheme, see 'Instructions for Authors', *J. Chem. Soc., Perkin Trans. 2*, available *via* the RSC web page (http://www.rsc.org/authors). Any request to the CCDC for this material should quote the full literature citation and the reference number 188/160. See http://www.rsc.org/suppdata/p2/1999/975/ for crystallographic files in .cif format.

‡ Fluorescence spectra for $\mathbf{L^1}$ at various Zn^{II} concentrations are available as supplementary data (SUPPL. NO. 57508, pp. 1) from the British Library. For details of the Supplementary Publications Scheme, see 'Instructions for Authors', *J. Chem. Soc., Perkin Trans. 2*, available *via* the RSC web page (http://www.rsc.org/authors). For direct electronic access see http://www.rsc.org/suppdata/p2/1999/975/.

Table 1 Crystallographic data for $\mathbf{1}\cdot 2H_2O$ and $\mathbf{2}\cdot 2CHCl_3$

	$\mathbf{1}\cdot 2H_2O$	$\mathbf{2}\cdot 2CHCl_3$
Formula	$C_{104}H_{76}N_8O_{18}S_4Cu_4$	$C_{54}H_{38}N_4O_6Cl_6Cu_2$
M	2108.21	1178.73
Crystal system	Monoclinic	Monoclinic
Space group	$P2_1/c$	$C2$
Unit cell dimensions	$a = 18.026(2)$ Å	$a = 17.198(3)$ Å
	$b = 23.450(3)$ Å	$b = 14.079(2)$ Å
	$c = 22.744(2)$ Å	$c = 13.644(3)$ Å
	$\beta = 90.299(9)°$	$\beta = 112.801(11)°$
U/Å^3	9613.6(2)	3045.5(9)
Z	4	2
T/K	173(2)	213(2)
λ(Mo-Kα)	0.71073 Å	0.71073 Å
D_c/g cm^{-3}	1.457	1.285
μ/mm^{-1}	1.029	1.305
F(000)	4240	998
Crystal size/mm	0.5 × 0.3 × 0.25	0.5 × 0.3 × 0.2
θ range for data collection/°	2.07–25.000	2.18–27.49
Index ranges	$0 < h < 21, 0 < k < 27, -27 < l < 27$	$0 < h < 22, 0 < k < 18, -17 < l < 16$
Reflections collected	17487	3920
Independent reflections	16918 [R(int) = 0.0487]	3650 [R(int) = 0.0452]
Refinement method	Full matrix least-squares on F^2	Full matrix least-squares on F^2
Data/restraints/parameters	16859/0/1261	3613/1/326
Goodness-of-fit on F^2	1.021	1.070
Final $R1$,[a] $wR2$[b] [$I > 2\sigma(I)$]	0.0667, 0.1652	0.0548, 0.1439
R indices (all data)	0.1624, 0.2381	0.0828, 0.2027
Largest diff. peak and hole/e Å^{-3}	0.833, −0.380	1.133, −0.431

[a] $R1 = \Sigma||F_o| - |F_c||/\Sigma|F_o|$. [b] $wR2 = [\Sigma[w(F_o^2 - F_c^2)^2/\Sigma w(F_o^2)^2]]^{1/2}$, calc $w = 1/[\sigma^2(F_o^2) + (0.1011P)^2 + 0.2555P]$ for $\mathbf{1}\cdot 2H_2O$ and calc $w = 1/[\sigma^2(F_o^2) + (0.1077P)^2 + 0.3994P]$ for $\mathbf{2}\cdot 2CHCl_3$, where $P = (F_o^2 + 2F_c^2)/3$.

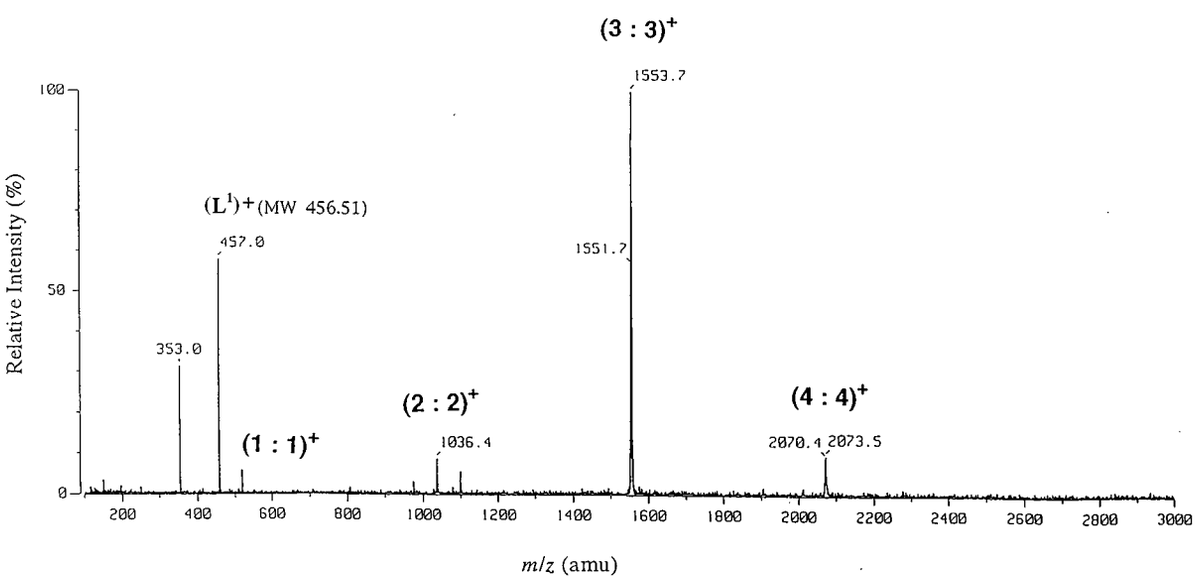

Fig. 2 ESI mass spectrum of a methanol solution of **1**.

nm, broad structureless band) is saturated at *ca.* $[Zn^{II}]/[\mathbf{L}^1] = 2$. No fluorescence enhancement was observed in other metal complex formation. The heavy metal ions such as Cu^{II} have been known to act as quenchers. On the other hand, the Cu^{II}–$\mathbf{L}^6$ and Zn^{II}–$\mathbf{L}^6$ systems show only the formation of a 1:1 ratio complex as judged by the presence of clear isosbestic points and the saturation in absorbance (λ_{obs} = 375 and 400 nm) at $[Cu^{II}]/[\mathbf{L}^6]$ and $[Zn^{II}]/[\mathbf{L}^6] = 1$.

Mass spectra of the Cu^{II}–L^1 complex

In an earlier stage of our investigations, we anticipated the formation of a metal-assisted self-assembled structure for the $Cu^{II}:\mathbf{L}^1 = 2:2$ type. Field desorption (FD) mass spectral data at m/z = 1035 support our expectation of the presence of a 2:2 ($Cu^{II}:\mathbf{L}^1$) self-assembling complex.[15] The isotopic patterns observed for this species are in good agreement with the calculated composition. A positive FAB mass spectrum at m/z = 1037 (NBA matrix) also indicates the presence of the relatively abundant $(2:2)^+$ species. However, the molecular ion peak for the $(3:3)^+$ species is also observed at m/z = 1553.

Electrospray ionization mass spectrometry (ESI-MS) has proved to be a mild ionization method for the characterization of many systems such as proteins, oligonucleotides, and coordination compounds.[16] Since no energy is required to ionize the sample, ESI-MS with no matrix is suitable to investigate the weak supramolecular species in solution.[17] Fig. 2 shows the positive ESI-MS (MeOH–trace $CHCl_3$) for **1**.

The relatively weak peaks at m/z = 518.0, 1036 and 2073.5 are assignable to $(Cu^{II}:\mathbf{L}^1)^+ = (1:1)^+$, $(2:2)^+$, and $(4:4)^+$ aggregate species. Comparison of the ESI-MS peak strength among

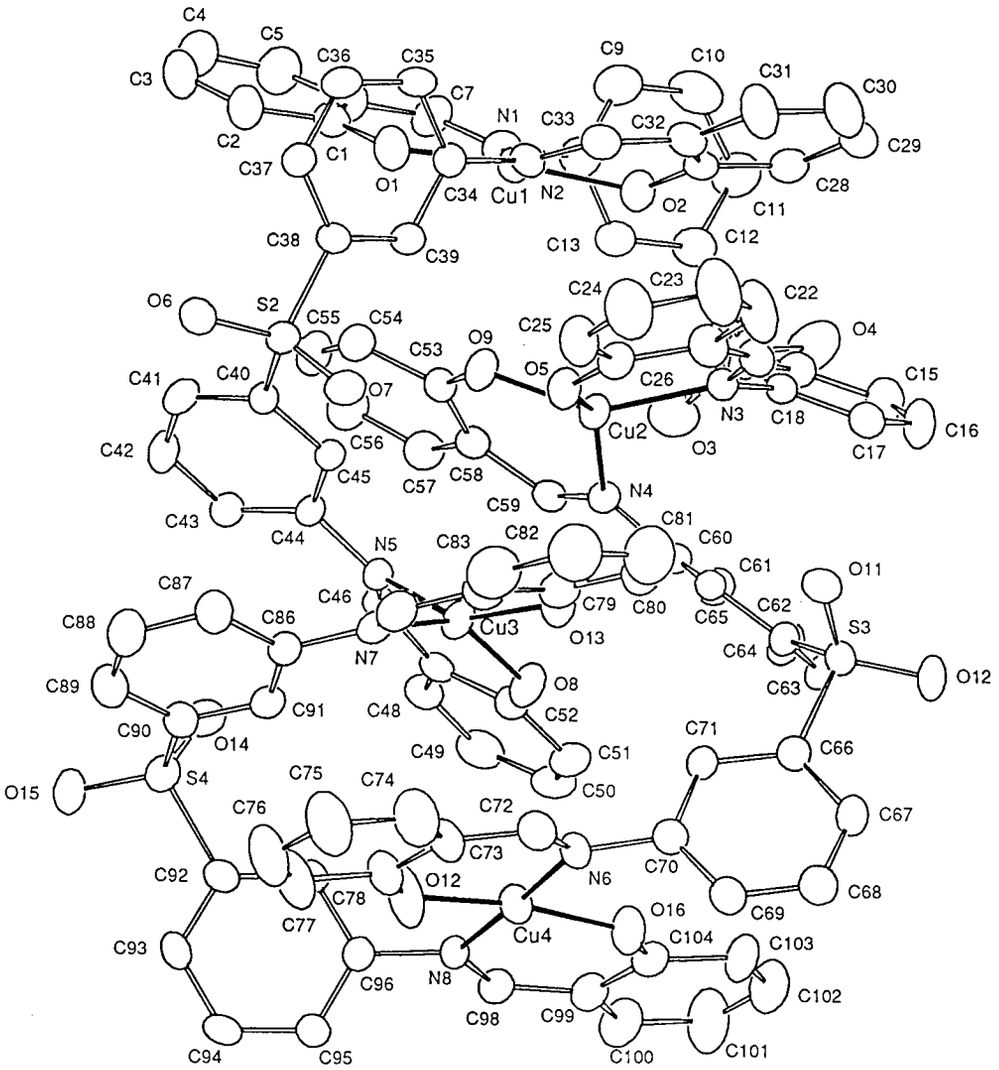

Fig. 3 X-Ray crystal structure for **1**.

the self-assembling species provides clearly the degree of distribution in the aggregates. It is noteworthy that in methanol solution a primary trinuclear $(3:3)^+$ species corresponding to $[\mathbf{L}^1\mathrm{H}_{-2}\text{–}\mathrm{Cu}^{\mathrm{II}}]_3$ is observed at 1553.7.

X-Ray crystal structure of the $\mathbf{L}^1$–$\mathrm{Cu}^{\mathrm{II}}$ complex, 1

Contrary to our expectations,[15] the crystal diffraction study of **1** confirms the formation of the tetranuclear ($\mathrm{Cu}^{\mathrm{II}}:\mathbf{L}^1 = 4:4$) structure with a double-helical motif as shown in Fig. 3. The neutral complex **1** contains four $\mathrm{Cu}^{\mathrm{II}}$ ions and four ligands $\mathbf{L}^1\mathrm{H}_{-2}$. Selected bond lengths and angles are presented in Table 2. A significant feature of this structure is the presence of π–π and CH–π aromatic interactions at 3.2–3.9 Å between several spacer groups (-$C_6H_4SO_2C_6H_4$-), resulting in the doubly helical and stacking structure. The Corey–Pauling–Koltun (CPK) representation shown in Fig. 4 indicates clearly the function of multiple π–π and CH–π aromatic interactions in **1**. As pointed out by some authors,[18] overlap of the aromatic ligands resulting in π-stacking interactions, although not necessarily a main controlling factor in the structure, must provide some additional degree of stabilization of the self-assembled species.

Each $\mathrm{Cu}^{\mathrm{II}}$ ion such as Cu1 (square-planar, SP), Cu2 (distorted tetrahedral, T_d), Cu3 (T_d), and Cu4 (SP) is coordinated by two *N*,*O*-bidentate sites from two different ligands. Each ligand, abbreviated as $\mathbf{L}^1$(1)/C1–C26, $\mathbf{L}^1$(2)/C27–C52, $\mathbf{L}^1$(3)/C53–C78, and $\mathbf{L}^1$(4)/C79–C104, interacts with two $\mathrm{Cu}^{\mathrm{II}}$ ions with a different coordination geometry.

Fig. 5 shows two main MM2-optimized conformations of ligand $\mathbf{L}^1$. These conformers are similar to those of the two types of conformation of $\mathbf{L}^1$ found in the tetranuclear double helical complex **1** in Fig. 3. Thus, the ligand conformation of $\mathbf{L}^1$(1)

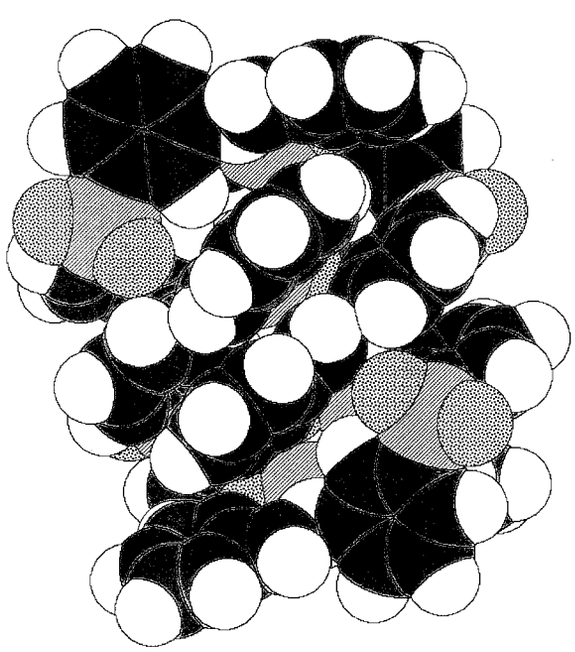

Fig. 4 Space-filling representation of **1**.

Table 2 Selected bond lengths (Å) and angles (°) for $(L^1H_{-2}Cu^{II})_4$ **1** with esds in parentheses

1			
Cu(1)–O(1)	1.889(5)	Cu(2)–O(5)	1.891(5)
Cu(1)–O(2)	1.903(5)	Cu(2)–O(9)	1.898(5)
Cu(1)–N(2)	1.999(6)	Cu(2)–N(3)	1.983(6)
Cu(1)–N(1)	2.024(6)	Cu(2)–N(4)	1.990(5)
Cu(3)–O(13)	1.871(5)	Cu(4)–O(12)	1.858(6)
Cu(3)–O(8)	1.879(5)	Cu(4)–O(16)	1.875(5)
Cu(3)–N(7)	1.968(6)	Cu(4)–N(6)	1.990(6)
Cu(3)–N(5)	1.979(5)	Cu(4)–N(8)	1.997(6)
C(7)–N(1)	1.282(9)	C(33)–N(2)	1.288(9)
C(20)–N(3)	1.301(9)	C(59)–N(4)	1.300(8)
C(46)–N(5)	1.311(8)	C(72)–N(6)	1.284(9)
C(85)–N(7)	1.315(9)	C(98)–N(8)	1.296(9)
O(1)–Cu(1)–O(2)	174.9(2)	O(5)–Cu(2)–O(9)	89.6(2)
O(1)–Cu(1)–N(2)	88.1(2)	O(5)–Cu(2)–N(3)	94.3(2)
O(2)–Cu(1)–N(2)	90.6(2)	O(9)–Cu(2)–N(3)	147.2(2)
O(1)–Cu(1)–N(1)	90.6(2)	O(5)–Cu(2)–N(4)	148.8(2)
O(2)–Cu(1)–N(1)	91.4(2)	O(9)–Cu(2)–N(4)	93.9(2)
N(2)–Cu(1)–N(1)	171.4(2)	N(3)–Cu(2)–N(4)	99.2(2)
O(13)–Cu(3)–O(8)	89.2(2)	O(12)–Cu(4)–O(16)	170.4(3)
O(13)–Cu(3)–N(7)	94.8(2)	O(12)–Cu(4)–N(6)	91.1(2)
O(8)–Cu(3)–N(7)	144.6(2)	O(16)–Cu(4)–N(6)	88.9(2)
O(13)–Cu(3)–N(5)	148.7(2)	O(12)–Cu(4)–N(8)	88.6(2)
O(8)–Cu(3)–N(5)	94.2(2)	O(16)–Cu(4)–N(8)	91.8(2)
N(7)–Cu(3)–N(5)	100.1(2)	N(6)–Cu(4)–N(8)	177.6(2)
C(12)–S(1)–C(14)	104.4(4)	C(40)–S(2)–C(38)	106.4(3)
C(64)–S(3)–C(66)	107.7(3)	C(92)–S(4)–C(90)	107.0(4)

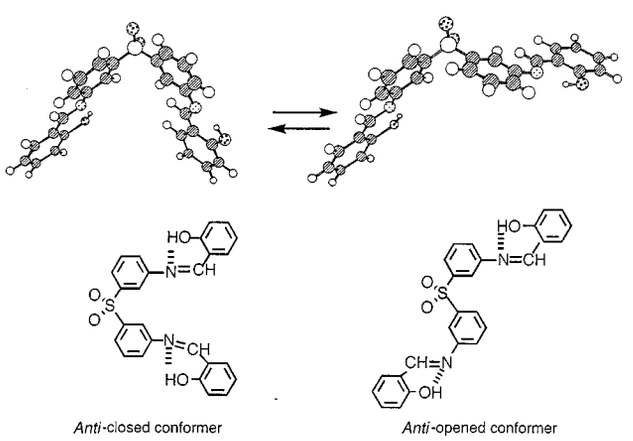

Fig. 5 Two main conformers of ligand L^1. $L^1(1)$ and $L^1(4)$ adopt the *anti*-closed conformer and $L^1(2)$ and $L^1(3)$ the *anti*-opened conformer.

ligated to Cu1 and Cu2 is similar to the *anti*-closed conformer[5b,19] in Fig. 5 and that of $L^1(4)$ coordinated to Cu3 and Cu4 also has the *anti*-closed conformation. On the other hand, the ligands $L^1(2)$ and $L^1(3)$ have been proved to have the *anti*-opened conformation. Judging from the E_{steric} values of the *anti*-closed conformer ($E_{steric} = -27.58$ kcal mol^{-1}) and the *anti*-open conformer ($E_{steric} = -27.16$ kcal mol^{-1}) of L^1, little energetical difference is required between the two conformational states. The theoretical interatomic O···O distances of the two hydroxy groups for the *anti*-closed and *anti*-open conformer of L^1 are estimated to be 9.226 Å and 11.221 Å, respectively. The experimental O···O distances (5.121 Å, 5.017 Å and 7.817 Å, 8.500 Å) determined from the X-ray crystal structure of **1** are appreciably smaller than the theoretical values. This result indicates that the X-ray structure for **1** is more compressed along the long axis of the tetranuclear structure than the MM2 structure for **1** owing to the presence of the aromatic stacking interactions. The selection of the *anti*-closed or *anti*-opened conformer by Cu^{II} ion seems to operate spontaneously in order to construct the final structure of **1**.

The four Cu^{II} ions with SP and T_d geometry are almost in plane and have a rhombic arrangement with Cu···Cu distances in the range of 4.08–7.66 Å (Scheme 2). The sum of

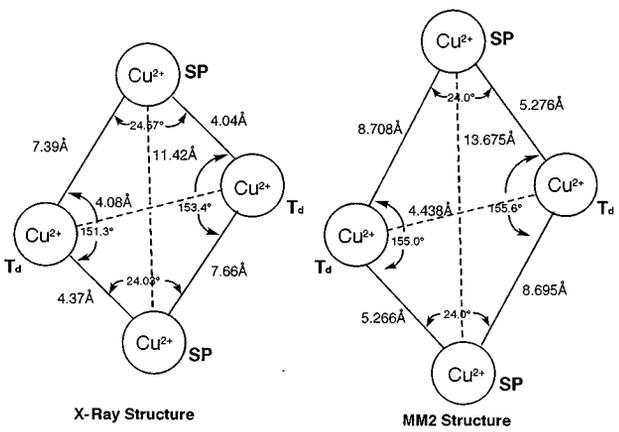

Scheme 2

the interior angles (353.3°) is comparable with that of the MM2 structure (358.6°). A more symmetrical arrangement of the four Cu^{II} ions is observed in the MM2 minimized structure.[20]

Other metal ions such as Zn^{II}, Ni^{II}, and Co^{II} appear to form the $(1:1)_\infty$ polymeric species which are insoluble in most organic solvents.[5b] Therefore, the formation of the double-helical tetranuclear structure could be ascribed to two factors: (1) the loose geometrical preference for SP or pseudo T_d of Cu^{II} ion and (2) the flexible conformation around the spacer group in L^1. Perhaps the ability of Cu^{II} to adopt both SP (Jahn–Teller effect) and pseudo T_d geometries would be the primary factor for formation of the tetranuclear structure. While tetrahedral coordination to Zn^{II} and Co^{II} is common, SP coordination is not, so a structure like the tetranuclear Cu^{II} complex (which requires two SP metal centers) is not possible. Thus the SP geometry seems to function as the end code for the helical winding program. Furthermore, the aromatic stacking interactions between the spacer groups would also play an important role in determining the final tunable structure with a double-helix motif.

Scheme 3 shows the proposed mechanism for the self-assembly process of eight components of Cu^{II} and L^1 into the tetranuclear supramolecular species **1** in solution. The synthetic conditions at a mole ratio of $Cu^{II}:L^1 = 1:1$ lead to the formation of the 1:1 species (step (a)). More aggregate (acyclic or cyclic) species which were detected by mass spectrometry may be formed in the subsequent steps (b) and (c) in order to complete the coordination site around the Cu^{II} center. Aromatic π–π and CH–π interactions would play an important role in these steps to create the tunable supramolecular architecture. In step (d), the final species is selected as the crystallized form from the various factors such as solvent, crystal packing force, and counter anion.[21] It appears that the most abundant species in solution is the 3:3 complex as shown in Fig. 2. The isolation of the 4:4 complex as a solid does not mean that this is the most stable species in solution. Therefore the representation of the 3:3 species in Scheme 3 would be quite appropriate.

Solution species and solid-state structure of the L^6–Cu^{II} complex

The L^6–Cu^{II} system has a similar potential for the construction of a supramolecular motif such as the double-helical structure which was found in the L^1–Cu^{II} system. A color change from colorless to pale yellow was observed when the Cu^{II} ion was added to the L^6 ethanol solution (Fig. 6). The intensity at 400

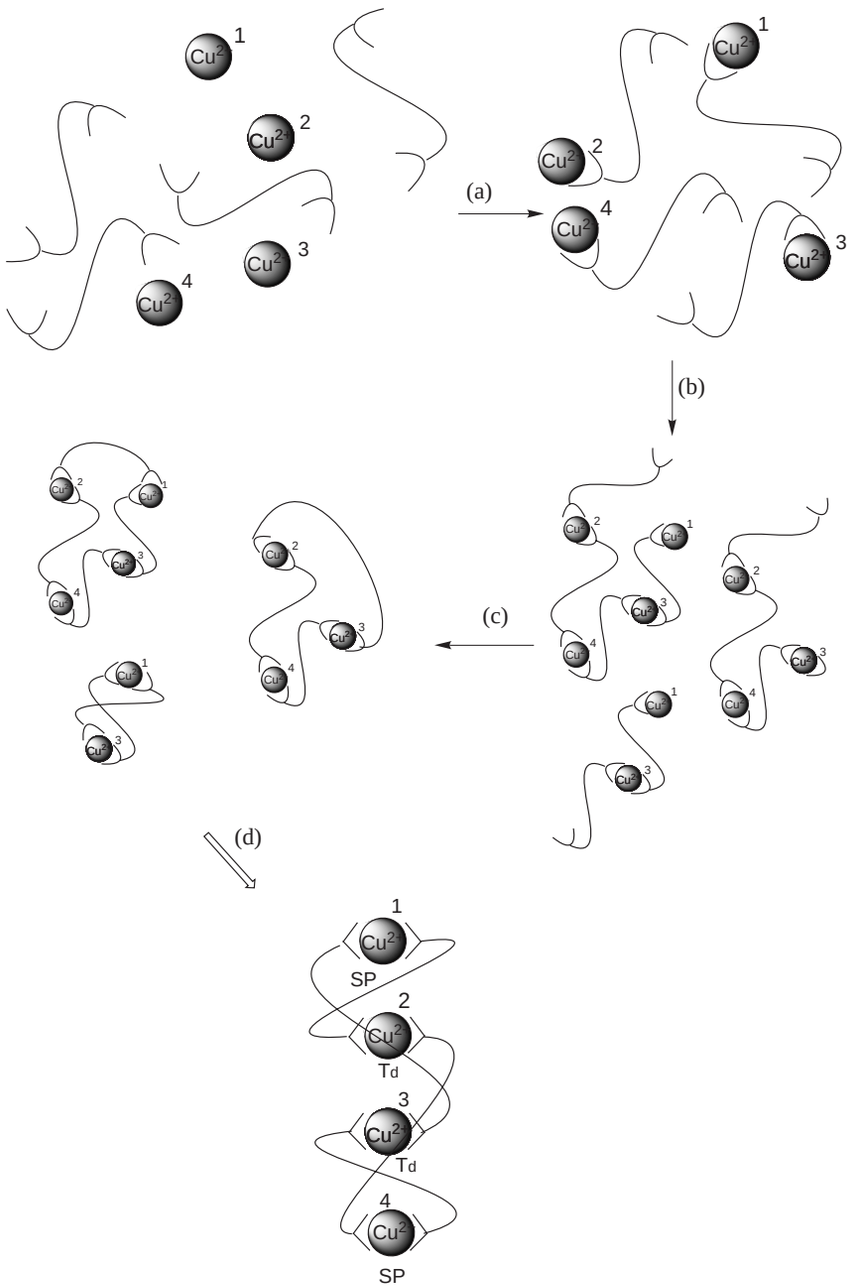

Scheme 3

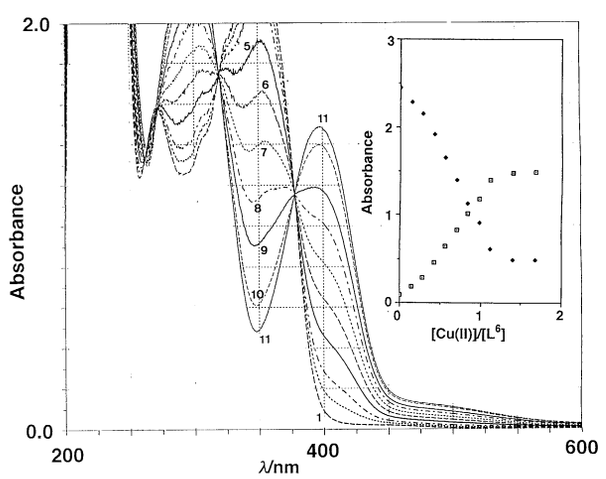

Fig. 6 Absorption spectral change of ligand $\mathbf{L^6}$ in ethanol upon addition of $Cu(CH_3COO)_2{\cdot}H_2O$. $[\mathbf{L^6}] = 6.49 \times 10^{-5}$ mol dm^{-3}. $[Cu^{II}] = 0$, 0.898, 1.796, 2.694, 3.592, 4.49, 5.39, 6.29, 7.18, 8.98, 10.78, 12.57, 14.37, 16.16, 17.96 $\times 10^{-5}$ mol dm^{-3}.

nm increased, whereas that at 350 nm decreased. The presence of some clear isosbestic points and the molar ratio plot demonstrate the formation of a 1 : 1 molar ratio complex.

The ESI-MS shown in Fig. 7 displays several characteristic peaks for the $\mathbf{L^6}$: Cu^{II} = 2 : 2, 3 : 3, and 4 : 4 species. The most abundant species is the 2 : 2 species at m/z = 941.1 in this system. The weak peaks corresponding to higher degrees of oligomers such as the 3 : 3 and 4 : 4 species may be related to the decrease in stability. The CPK molecular considerations suggest that the 4,4′-position of the azomethine (-CH=N-) at the diphenyl ether moiety in $\mathbf{L^6}$ lowers the stability of the 3 : 3 and 4 : 4 species.

The X-ray structural analysis supports clearly the idea that the $\mathbf{L^6}$–Cu^{II} complex has a dinuclear structure with the double-helix as a supramolecular motif in the solid state (Fig. 8 and Table 3). The *N*,*O*-coordination sites from two different ligands bind to one Cu^{II} ion. Two ligands are coordinated to Cu^{II} in a strain-free manner, as judged by observing the normal C(11)–O(3)–C(24) bond angle, 116.7(6)°. Slightly longer Cu–O (1.899(4) and 1.901(5) Å) and shorter Cu–N (1.959(5) and 1.967(6) Å) bond lengths as compared with the other Schiff base planar Cu^{II} complex (1.874 Å for Cu–O and 2.009 Å for

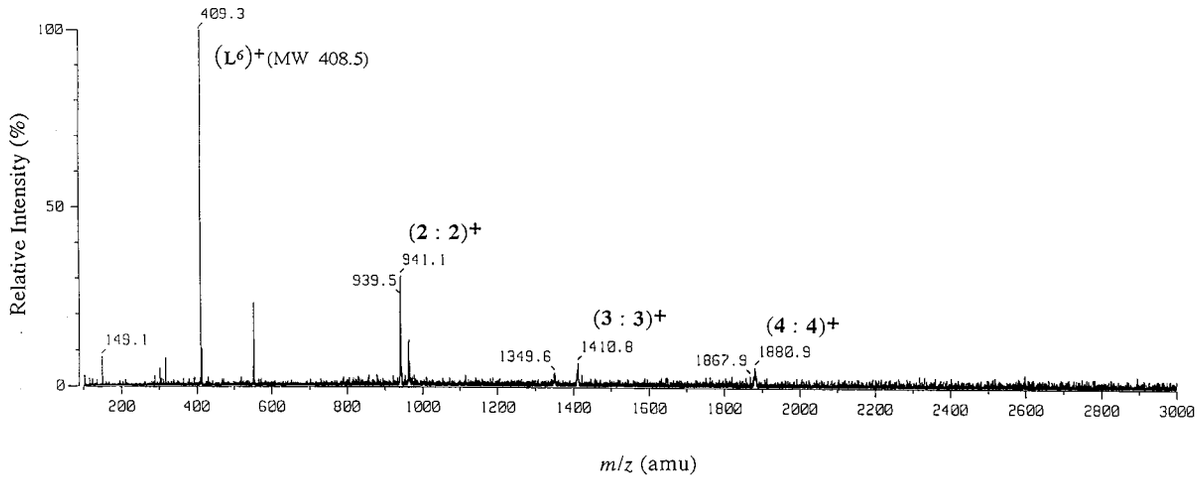

Fig. 7 ESI mass spectrum of a methanol solution of **2**.

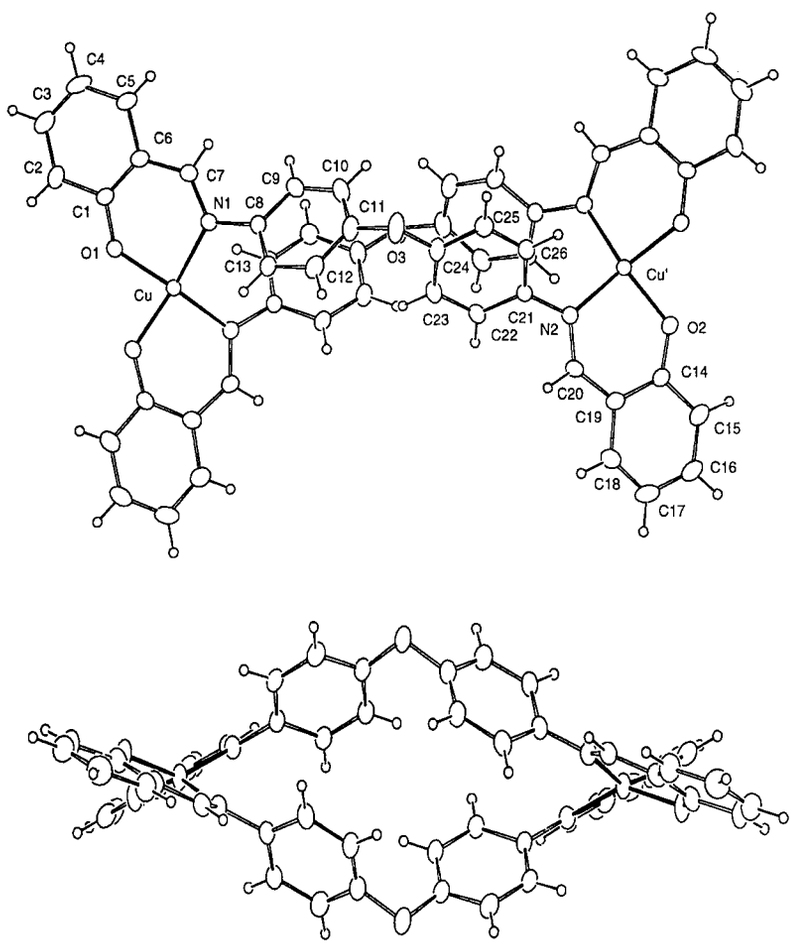

Fig. 8 X-Ray crystal structure for **2**.

Cu–N)[22] are observed. The geometry around the two Cu^{II} ions is described as distorted tetrahedral, as shown in the side view of Fig. 8. The aromatic π–π and CH–π interactions operating between the bridging groups (-$C_6H_4OC_6H_4$-) of two $\mathbf{L}^6$ ligands may be one of the crucial factors in building the double-helical structure. Furthermore, since the 4,4′-position of -CH=N- at the diphenyl ether moiety in $\mathbf{L}^6$ may prevent the fully-parallel stacking between the spacer groups of the interligand, the binuclear species are predominantly formed in solution and as solids.

Other Cu^{II} complexes of L^2–L^5

Since X-ray characterizations of most of the Cu^{II} complexes investigated here have been unavailable due to the poorly crystalline powders, mass spectrometry is a useful method to detect the supramolecular species in solution. The ESI mass spectra of $\mathbf{L}^5$–Cu^{II} show clearly the formation of $(2:2)^+$, $(3:3)^+$, and $(4:4)^+$ species as shown in Fig. 9. On the other hand, polycrystalline solids were obtained in the $\mathbf{L}^2$–Cu^{II} complex. The formation of $(2:2)^+$ species occurs in solution as judged from the ESI spectra. The ESI mass spectra of $\mathbf{L}^3$–Cu^{II} and $\mathbf{L}^4$–Cu^{II} show only the peaks due to the $\mathbf{L}^+$ and $(Cu^{II}:\mathbf{L} = 1:1)^+$ species. Perhaps the formation of 2:2, 3:3, and 4:4 species may be retarded by the steric hindrance of the -OCH_3 group in $\mathbf{L}^3$–Cu^{II} and the electron withdrawing effect of the *para* -SO_2- group in $\mathbf{L}^4$–Cu^{II}. Smaller uv–vis spectral changes of these systems support these inhibition effects.

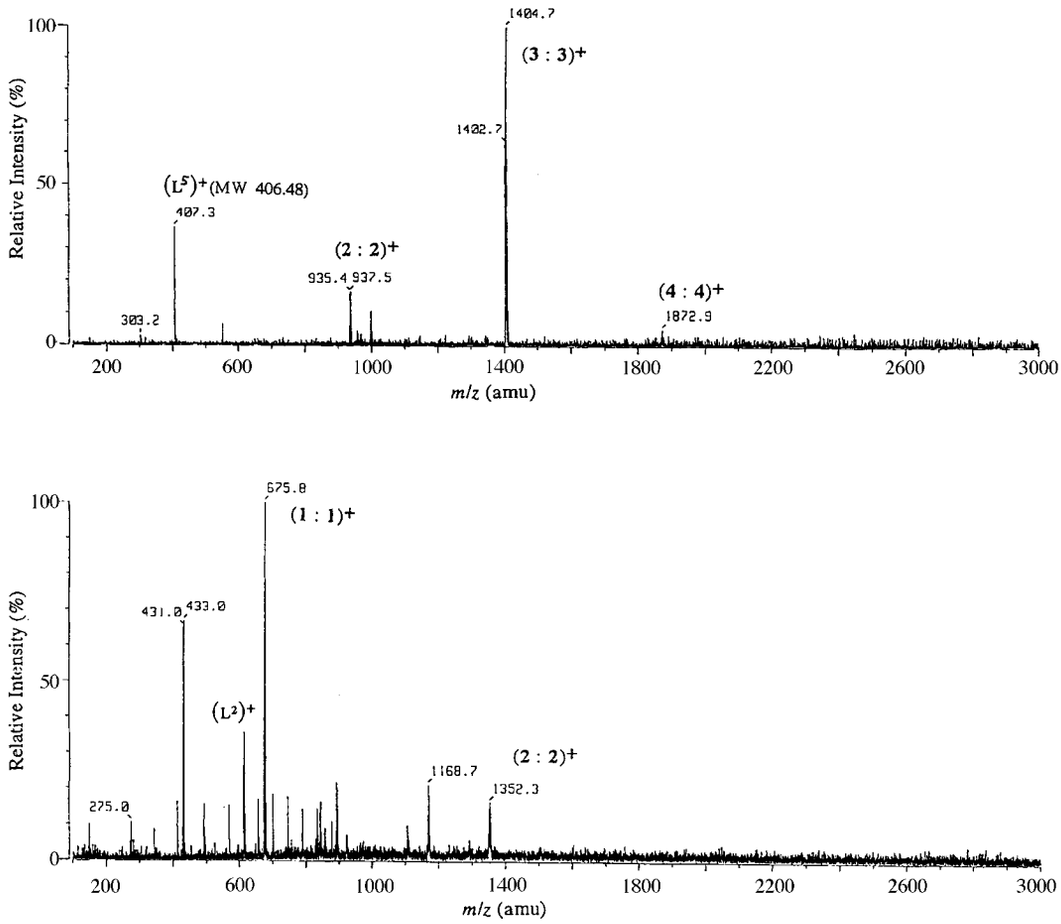

Fig. 9 ESI mass spectra of $\mathbf{L}^5$–Cu^{II} and $\mathbf{L}^2$–Cu^{II} complexes.

Table 3 Selected bond lengths (Å) and angles (°) for $(\mathbf{L}^6H_{-2}Cu^{II})_2$ **2** with esds in parentheses

2			
Cu–O(1)	1.899(4)	Cu–O(2)	1.901(5)
Cu–N(2)	1.959(5)	Cu–N(1)	1.967(5)
N(1)–C(7)	1.309(7)	N(2)–C(20)	1.313(8)
N(1)–C(8)	1.428(7)	N(2)–C(21)	1.433(7)
O(1)–C(1)	1.295(7)	O(2)–C(14)	1.295(9)
O(3)–C(24)	1.374(8)	O(3)–C(11)	1.409(8)
O(1)–Cu–O(2)	89.2(2)	O(1)–Cu–N(2)	145.7(2)
O(2)–Cu–N(2)	94.5(2)	O(1)–Cu–N(1)	93.9(2)
O(2)–Cu–N(1)	148.0(2)	N(2)–Cu–N(1)	100.4(2)
C(1)–O(1)–Cu	128.6(4)	C(14)–O(2)–Cu	127.7(4)
C(24)–O(3)–C(11)	116.7(5)	C(7)–N(1)–C(8)	115.2(5)
C(7)–N(1)–Cu	122.6(4)	C(8)–N(1)–Cu	122.1(4)
C(20)–N(2)–C(21)	116.5(5)	C(20)–N(2)–Cu	122.6(4)
C(21)–N(2)–Cu	120.7(4)	O(1)–C(1)–C(6)	123.6(6)
N(1)–C(7)–C(6)	126.7(6)	O(2)–C(14)–C(19)	124.3(6)
N(2)–C(20)–C(19)	127.7(6)		

Conclusion

We have presented the structural characterization of two copper(II) complexes of bis-*N*,*O*-bidentate Schiff base ligands, $\mathbf{L}^1$ and $\mathbf{L}^6$. The utilization and combination of Cu(II) and the bis-*N*,*O*-bidentate Schiff base having the flexible spacer group allow the facile formation of the tetranuclear and dinuclear Cu(II) complexes containing the double-helical motif. The weak π–π and CH–π aromatic interactions between the spacer groups and the flexible geometry of the Cu(II) ion would play an important role in determining the supramolecular structure.

Acknowledgements

We thank the GC-MS and NMR Laboratory, Faculty of Agriculture, Hokkaido University for the measurements of FAB MS and ESI-MS spectra.

References

1 N. Yoshida and K. Hayashi, *J. Chem. Soc., Perkin Trans. 2*, 1994, 1285; A. V. Eliseev and H.-J. Schneider, *J. Am. Chem. Soc.*, 1994, **116**, 6081; N. Yoshida and Y. Fujita, *J. Phys. Chem.*, 1995, **99**, 3671; N. Yoshida, *J. Chem. Soc., Perkin Trans. 2*, 1995, 2249; N. Ito, N. Yoshida and K. Ichikawa, *J. Chem. Soc., Perkin Trans. 2*, 1996, 965.

2 (*a*) D. Philp and J. F. Stoddart, *Angew. Chem., Int. Ed. Engl.*, 1996, **35**, 1154; (*b*) J.-M. Lehn, *Supramolecular Chemistry*, VCH, Weinheim, 1995; (*c*) F. Vögtle, *Supramolecular Chemistry: An Introduction*, Wiley, New York, 1991; (*d*) *Frontiers in Supramolecular Organic Chemistry and Photochemistry*, ed. H.-J. Schneider and H. Dürr, VCH, Weinheim, 1991.

3 (*a*) H. Adams, F. J. Carver, C. A. Hunter, J. C. Morales and E. M. Seward, *Angew. Chem., Int. Ed. Engl.*, 1996, **35**, 1542 and references therein; (*b*) M. Nishio, Y. Umezawa, M. Hirota and Y. Takeuchi, *Tetrahedron*, 1995, **51**, 8665; I. Dance and M. Scudder, *Chem. Eur. J.*, 1996, **2**, 481.

4 (*a*) J. S. Fleming, E. Psillakis, S. M. Couchman, J. C. Jeffery, J. A. McCleverty and M. D. Ward, *J. Chem. Soc., Dalton Trans.*, 1998, 537; (*b*) J. S. Fleming, K. L. V. Mann, C.-A. Carraz, E. Psillakis, J. C. Jeffery, J. A. McCleverty and M. D. Ward, *Angew. Chem., Int. Ed. Engl.*, 1998, **37**, 1279; (*c*) E. Psillakis, J. C. Jeffery, J. A. McCleverty and M. D. Ward, *Chem. Commun.*, 1997, 479; C. M. Hartshorn and P. J. Steel, *J. Chem. Soc., Dalton Trans.*, 1998, 3927.

5 (*a*) N. Yoshida and K. Ichikawa, *Chem. Commun.*, 1997, 1091; (*b*) N. Yoshida, H. Oshio and T. Ito, *Chem. Commun.*, 1998, 63.

6 P. N. W. Baxter, H. Sleiman, J.-M. Lehn and K. Rissanen, *Angew. Chem., Int. Ed. Engl.*, 1997, **36**, 1294; B. Mohr, M. Weck, J.-P. Sauvage and R. H. Grubbs, *ibid.*, 1997, **36**, 1308; E. C.

Constable, F. R. Heirtzler, M. Neuburger and M. Zehnder, *Chem. Commun.*, 1996, 933.
7 V. C. M. Smith and J.-M. Lehn, *Chem. Commun.*, 1996, 2733; E. C. Constable, M. Neuburger, D. R. Smith and M. Zehnder, *Chem. Commun.*, 1996, 1917; R. W. Saalfrank, R. Harbig, J. Nachtrab, W. Bauer, K.-P. Zeller, D. Stalke and M. Teichert, *Chem. Eur. J.*, 1996, **2**, 1363; M. Albrecht, H. Röttele and P. Burger, *Chem. Eur. J.*, 1996, **2**, 1264.
8 E. J. Enemark and T. D. P. Stack, *Angew. Chem.*, *Int. Ed. Engl.*, 1998, **37**, 932; M. Albrecht and O. Blau, *Chem. Commun.*, 1997, 345; M. Meyer, B. Kersting, R. E. Powers and K. N. Raymond, *Inorg. Chem.*, 1997, **36**, 5179.
9 G. Hopfgartner, C. Piguet and J. D. Henion, *J. Am. Soc. Mass Spectrom.*, 1994, **5**, 748.
10 P. Baxter, J.-M. Lehn, A. De Cian and J. Fischer, *Angew. Chem.*, *Int. Ed. Engl.*, 1994, **32**, 69.
11 M. J. Hannon, C. L. Painting and W. Errington, *Chem. Commun.*, 1997, 307; C. M. Hartshorn and P. J. Steel, *Chem. Commun.*, 1997, 541; P. Losier and M. J. Zaworotko, *Angew. Chem.*, *Int. Ed. Engl.*, 1996, **35**, 2779; C. A. Hunter, *Angew. Chem.*, *Int. Ed. Engl.*, 1995, **34**, 1079; P. J. Stang and K. Chen, *J. Am. Chem. Soc.*, 1995, **117**, 1667; M. Fujita, J. Yazaki and K. Ogura, *J. Am. Chem. Soc.*, 1990, **112**, 5645.
12 O. Mamula, A. Zelewsky and G. Bernardinelli, *Angew. Chem.*, *Int. Ed. Engl.*, 1998, **37**, 290; P. L. Jones, K. J. Byrom, J. C. Jeffery, J. A. McCleverty and M. D. Ward, *Chem. Commun.*, 1997, 1361; D. Funeriu, J.-M. Lehn, G. Baum and D. Fenske, *Chem. Eur. J.*, 1997, **3**, 99; B. Hasenknopf, J.-M. Lehn, B. O. Kneisel, G. Baum and D. Fenske, *Angew. Chem.*, *Int. Ed. Engl.*, 1996, **35**, 1838.
13 N. Yoshida, N. Ito and K. Ichikawa, The 46th Symposium on Coordination Chemistry of Japan, Osaka, Japan, 1996, 46, 91.
14 N. Yoshida and M. Fujimoto, *Bull. Chem. Soc. Jpn.*, 1976, **49**, 1557.
15 The energy-minimized structure of the $2:2 = Cu^{II}:\mathbf{L}^{1}$ complex calculated by MM2 molecular mechanics shows that the steric energy of the 2:2 complex with SP coordination geometry ($E_{steric} = 8.662$ kcal mol^{-1}) is considerably larger than the 2:2 complex with T_d geometry ($E_{steric} = -32.212$ kcal mol^{-1}). See also ref. 24.
16 J. B. Fenn, M. Mann, C. K. Meng, S. F. Wong and C. M. Whitehouse, *Science*, 1989, **246**, 64; V. Katta, S. K. Chowdhury and B. T. Chait, *J. Am. Chem. Soc.*, 1990, **112**, 5348; F. Bitsch, C. O. Dietrich-Buchecker, A. K. Klémiss, J.-P. Sauvage and A. Van Dorsselaer, *J. Am. Chem. Soc.*, 1991, **113**, 4023; J. T. Stults and J. C. Marsters, *Rapid Commun. Mass Spectrom.*, 1991, **5**, 359.
17 K. A. Hirsch, S. R. Wilson and J. S. Moore, *J. Am. Chem. Soc.*, 1997, **119**, 10401; M. Przybylsky and M. O. Glocker, *Angew. Chem.*, *Int. Ed. Engl.*, 1996, **35**, 806; K. Wang, X. Han, R. W. Gross and G. W. Gokel, *J. Am. Chem. Soc.*, 1995, **117**, 7680; K. C. Russell, E. Leize, A. V. Dorsselaer and J.-M. Lehn, *Angew. Chem.*, *Int. Ed. Engl.*, 1995, **34**, 209.
18 D. A. Bardwell, J. C. Jeffery and M. D. Ward, *J. Chem. Soc.*, *Dalton Trans.*, 1995, 3071.
19 Although $\mathbf{L}^{1}$ could adopt many conformational isomers, molecular mechanics (MM2) calculations revealed two minimum-energy structures such as *anti*-closed and *anti*-opened conformations. These two isomers have almost the same steric energy. Other minimum-energy structures: *syn*-opened ($E_{steric} = -27.4973$ kcal mol^{-1}) and *syn*-closed ($E_{steric} = -28.820$ kcal mol^{-1}) conformers. N. L. Allinger, *J. Am. Chem. Soc.*, 1977, **99**, 8127.
20 Cache Ver. 3.5. See ref. 23. The fairly large steric energy ($E_{steric} = 739.54$ kcal mol^{-1}) calculated for the X-ray crystal structure indicates **1** has a strained conformation in the ligand unit. This large strain is mainly reflected in the large bond-stretch and dihedral energy. The CPK representation in Fig. 7 indicates that this compressed structure may be compensated for by the aromatic π–π and CH–π interactions. The more symmetrical MM2 structure has quite a small steric energy ($E_{steric} = -12.58$ kcal mol^{-1}).
21 P. N. W. Baxter, J.-M. Lehn and K. Rissanen, *Chem. Commun.*, 1997, 1323.
22 N. Yoshida, N. Ito and K. Ichikawa, *J. Chem. Soc.*, *Perkin Trans. 2*, 1997, 2387.

Paper 8/09743G